



King Saud University
Arabian Journal of Chemistry

www.ksu.edu.sa
www.sciencedirect.com



ORIGINAL ARTICLE

Cotton fabric loaded with ZnO nanoflowers as a photocatalytic reactor with promising antibacterial activity against pathogenic *E. coli*



Ambreen Ashar^a, Zeeshan Ahmad Bhutta^{b,*}, Muhammad Shoaib^c,
Nada K. Alharbi^d, Muhammad Fakhar-e-Alam^e, Muhammad Atif^f,
Muhammad Fakhar-e-Alam Kulyar^{g,*}, Ashar Mahfooz^h, Prerona Boruahⁱ,
Mohamed R. Eletmany^{a,j}, Fatimah A. Al-Saeed^{k,l}, Ahmed Ezzat Ahmed^{k,*}

^a TECS Department, Wilson College of Textiles, NC State University, Raleigh 27606, USA

^b Laboratory of Veterinary Immunology and Biochemistry, College of Veterinary Medicine, Chungbuk National University, Cheongju 28644, Republic of Korea

^c Key Laboratory of New Animal Drug Project, Gansu Province/Key Laboratory of Veterinary Pharmaceutical Development, Ministry of Agriculture and Rural Affairs/Lanzhou Institute of Husbandry and Pharmaceutical Sciences of the Chinese Academy of Agricultural Sciences, Lanzhou 730050, China

^d Department of Biology, College of Science, Princess Nourah bint Abdulrahman University, Riyadh 11671, Saudi Arabia

^e Department of Physics, GC University, Faisalabad 38000, Pakistan

^f Department of Physics and Astronomy, College of Science, King Saud University Riyadh 11451, Saudi Arabia

^g College of Veterinary Medicine, Huazhong Agricultural University, Wuhan 430070, China

^h Department of Clinical Medicine and Surgery, University of Agriculture Faisalabad, Pakistan

ⁱ D Y Patil Deemed to be University, Mumbai 400706, India

^j Chemistry Department, Faculty of Science, South Valley University, Qena 83523, Egypt

^k Department of Biology, College of Science, King Khalid University, Abha 61421, Saudi Arabia

^l Research Center for Advanced Materials Science (RCAMS), King Khalid University, Abha 61421, Saudi Arabia

Received 1 February 2023; accepted 12 June 2023

Available online 19 June 2023

KEYWORDS

ZnO;

Abstract Nanofinishing is the process by which ultrafine dispersion of nanomaterials is applied to a textile for the development of functionalities. The utilization of nanometal oxides as antimicrobial

* Corresponding authors.

E-mail addresses: zee@chungbuk.ac.kr (Z.A. Bhutta), fakharealam786@mail.hzau.edu.cn (M. Fakhar-e-Alam Kulyar), aabdelrahman@kku.edu.sa (A. Ezzat Ahmed).

Peer review under responsibility of King Saud University. Production and hosting by Elsevier.



<https://doi.org/10.1016/j.arabjc.2023.105084>

1878-5352 © 2023 The Author(s). Published by Elsevier B.V. on behalf of King Saud University. This is an open access article under the CC BY license (<http://creativecommons.org/licenses/by/4.0/>).

Nano flowers;
Cotton;
Antibacterial

agents have shown a substantial antimicrobial property in cotton. In the present study, previously synthesized powder containing ZnO nanoflowers (ZnO NFs) was characterized for morphology, surface composition, roughness, and charge using Transmission electron microscopy (TEM), Scanning transmission electron microscopy (STEM), Atomic force microscopy (AFM) and Zeta potential. Optical properties of crystalline ZnO were determined by Photoluminescence (PL), Diffused reflectance Spectroscopy (DRS), and bandgap energy determination. Highly crystalline, ZnO NFs bearing crystal defects and high surface charge were loaded onto the pristine cotton by a dip coating method using Triton X-100 as dispersant and iSys MTX fabric binder. The pristine cotton fabric of 125 g/m² was nano finished by loading 20,42 and 58 µg/cm² (1–3 dip cycles) ZnO NFs respectively. The loading of ZnO NFs onto the surface of cotton fabric was confirmed by SEM and used for antibacterial activity against *E. coli* as a photocatalytic reactor. The prepared samples were irradiated with a UV lamp of λ_{max} = 254 nm (15 min, 30 min, 45 min) and D65 artificial sunlight (60 min, 120 min, 180 min) to investigate their photocatalytic activity against pathogenic *E. coli* using modified Breed Smear's method. The minimum inhibitory concentration (MIC) and minimum bactericidal concentration (MBC) of ZnO NFs@ cotton were determined as 19.53 µg/ml and 39.06 µg/ml respectively after exposure to UV light. After exposure to sunlight MIC and MBC observed were higher i.e. 156.25 µg/ml and 312.5 µg/ml respectively showing lesser activity in sunlight as compared to ionizing UV radiations. To verify the photocatalytic activity, hydroxyl radicals generated by ZnO NFs@ cotton were also determined time-resolved PL on exposure to a UV lamp and D65 artificial sunlight. This nano-finished cotton is a promising candidate to be used as a medical textile with high antibacterial activity even after 20 washing cycles with only a 5% decrease in efficiency.

© 2023 The Author(s). Published by Elsevier B.V. on behalf of King Saud University. This is an open access article under the CC BY license (<http://creativecommons.org/licenses/by/4.0/>).

1. Introduction

The modernized textile industry observes relentless customer demand in the context of innovations in technology and the streaming of innovative products. Three generations in the development of smart textiles have been observed, first generation is termed as passive smart textiles capable of sensing changes in the environs regardless of adjustment in their responses (Shah et al., 2022). Nanofinishing is the procedure according to which the ultrafine dispersion of nanomaterials is impregnated to a textile material for the induction of some functionalities. The nanocoating of nanomaterials does not affect the aesthetic look and feel of the textile. In short, the traditional finishes of textiles are being replaced by nanofinishing-based functionalities especially those which are hard to be attained (Gokarneshan and Velumani 2018, Ghosh et al., 2020).

Textiles prepared by cellulosic fibers such as lyocell, cotton, viscose, and linen possess a greater susceptibility to being attacked by microbes like fungi, algae, protozoa, bacteria, and viruses during their life cycles (Ahmed et al., 2017, Bu et al., 2019, Saleem and Zaidi 2020). The infectious diseases caused by bacteria result in severe health issues globally drawing the attention of researchers. The lack of suitable vaccines are internationally suffering for humans e.g. the bacteria (*Shigella flexneri*) causing water contamination kills more than 212,438 people annually (Khalil et al., 2018).

In recent times, the enhancement in consciousness about health and hygiene regarding antimicrobial moieties has become an important prerequisite for clothes, medical, textiles and other household products. Recently, various nanometal oxides such as TiO₂, CuO, SiO₂, and ZnO and nanoparticles of metals like Ag, Au, Cu, and Ti have gained remarkable attention from research perspectives regarding antimicrobial agents (Naseem and Durrani 2021). Reports have revealed that nanomaterials having a high surface-to-volume ratio can contribute much higher antimicrobial activity comparative to customary antimicrobial agents.

The employment of nano metal oxides as antimicrobial moieties adhered to textiles inflicts a positive impact on fabrics. These functionalized cotton fibers demonstrated adequate antibacterial efficiency after much laundry washing items, rendering them suitable as medical

textiles (Ullah et al., 2014). Numerous antimicrobial moieties such as TiO₂ (Tudu et al., 2020), chitosan (Benltoufa et al., 2020), N-Halamine (Wang et al., 2022), Ag (Xu et al., 2019), Cu₂O (Ren et al., 2011) and metal/hemp fibers (Kostic et al., 2014) etc. have been impregnated onto the fibers and fabrics as antimicrobial agents. Nanomaterials-based antimicrobial textiles can be fabricated by adhering them to the fabrics employing chemical or physical methods (Sun et al., 2019). Moreover, the functionalized cotton showed a high density of nanoparticles on the cotton fabric yarn capable of showing substantial antibacterial activity (Patil et al., 2021).

Nano-materials Possessing antimicrobial properties that have been synthesized by diverse techniques, such as precipitation, electrospinning, hydrothermal and self-assembly methods (Muñoz-Bonilla and Fernández-García 2015). The morphology of nanostructures has been examined to affect their antibacterial property. The nanostructures impregnated on cotton fabrics having core corona morphology have been explored for self-cleaning and antibacterial function (Song et al., 2013).

Among all transition metal oxides, ZnO is a versatile material exhibiting a broad range of applications and it was also recorded as a safe material by the U.S. FDA (21CFR182.899). It can readily undergo redox reactions catalyzed by radiations, due to its characteristic electronic configuration regarding occupied, conduction band (CB), and a vacant valence band (VB).

The photo-generated charge carriers i.e. electrons and holes, upon irradiation, have the probability of recombination within picoseconds. On the other hand, they can react with other species such as O₂ and H₂O, adsorbed onto the surface of nanometal oxides. The ROS generated through the chain of redox reactions, such as OH•, H₂O₂, and superoxide O^{•−} are believed to destroy the bacterial cell into CO₂, H₂O, and other nontoxic minerals (Yemmireddy and Hung 2017, Bhutta et al., 2021).

In addition to the employment of UV as a radiation source, researchers are more inclined towards the use of natural sunlight. The global capacity of solar energy is 1575–49837 EJ/annum, almost three times greater than the total global consumption of energy 600 EJ/annum (Creutzig et al., 2017). Many attempts have been done to create solar active photocatalysts by morphology engineering and

bandgap tuning. Various inorganic semiconductor metal oxides and along with their hybrids and nanocomposite have been investigated to harvest solar energy for numerous functions such as the generation of energy and self-cleaning properties (Pirzada et al., 2019, Pirzada et al., 2021).

The properties of nanomaterials are observed to be robustly dependent on crystallinity, shape, size, phase composition, dispersion, etc. The morphology has especially the crucial role in sensors, photonics, optics, and solar cells to acquire high-quality modern devices (Flores et al., 2014, Sharma et al., 2019, BoopathiRaja and Parthibavarman 2020). Consequently, the photocatalytic activity of semiconductors is dependent on their morphology, particle size, and high surface area (Kanjwal et al., 2010, Barakat et al., 2013).

Since, aspect ratio, morphology, and surface area affect the antibacterial activity, it is important to synthesize nanomaterials having novel morphology with a greater number of adsorption sites (Wu et al., 2019). Despite of numerous benefits of the nanostructures, their main shortcoming is particle agglomeration due to high surface charge. However modern methodologies aid in the fabrication of desired dimensions of nanoparticles without using any stabilizers and surfactants (Kawasaki 2013). The anisotropic, multi-dimensional, and multi-compartmental nanoparticles having unique morphologies are the main attraction of extensive research. (Babayevska et al., 2022). The (3D) nanostructures which are fabricated by the secondary growth of 1D) and 2D nanostructures having designed morphology are termed as Superstructures". Since, 3D nanostructures possess high crystallinity, and stacked integrated arrangement, as compared to 1D and 2D nanostructures, ZnO superstructures are superior. (Desai et al., 2019).

In the present study, attempt has been made to fabricate functionalized cotton with antibacterial properties by loading a unique morphology bearing ZnO, as a photocatalyst. The Novelty of the work is the development of a new method for photocatalytic study regarding the antibacterial activity of 3D flower-shaped nanoparticles of ZnO, by the modification of Breed Smear's method. The importance of intrinsic crystal defects, surface charge, surface roughness, and optical properties of a photocatalyst towards antibacterial activity have been rarely described in the literature. The mechanism of bactericidal action of nanoflowers of ZnO has been investigated in the light of structural, optical, and surface properties. The durability of nano finishing was also determined to ensure the efficiency of ZnO NFs@ cotton as a reusable antibacterial agent against *E. coli*.

2. Materials and methods

2.1. Materials

ZnO nanoflowers (Powder) self-synthesized by precipitation method (Ashar 2016), Triton X¹⁰⁰ (Sigma-Aldrich, St. Louis, MO, USA), iSys MTX (CHT, Germany) fabric binder, Pristine cotton fabric of 125 g/m² obtained from National textile University, Faisalabad, Pakistan.

Nutrient broth, Nutrient Agar medium, and pathogenic *E. coli* strain were taken from the Institute of Microbiology, University of Agriculture Faisalabad, Pakistan. Muller Hinton agar and MacConkey agar were purchased from Huankai Microbial, Guangzhou, China.

2.2. Characterization of ZnO NFs

The ZnO powder obtained through precipitation reaction was characterized for morphology through SEM (Quanta 2500, FEG (USA) (Ashar et al., 2016), TEM, and HRTEM (JEOL 2 M 2100), for the surface composition of elements (STEM). The optical properties were determined by PL (F-320, Guang-

dong Technology Co., Ltd., Guangdong, China), DRS (Perkin Elmer Lambda 1050, Buckinghamshire, UK), and band gap energy. The surface roughness has been measured by AFM (Shimadzu WET-SPM 9600).

2.3. Loading of ZnO nanoflowers on cotton fabric

To 100 ml of distilled water, 0.060 g of Triton X¹⁰⁰ and 5 g of previously synthesized and published ZnO NFs powder were added (Ashar et al., 2016). The mixture was mechanically stirred for 30 min and ultrasonicated for 15 min after adding 4 g of MTX fabric binder. Untreated four cotton fabric pieces of 15 cm² were dipped into the prepared solution, padded, dried, and cured at 120 °C using a curing machine (National Textile University Faisalabad, Pakistan). The dipping and curing process was executed 1–3 times for pristine cotton. The Pieces of loaded cotton fabric were tagged as 1dip to 3 dips and cut into swatches of 1.5 cm² with a sterilized scissor. The nano-finished swatches were weighed on microbalance and saved in sterilized plastic bags. The control was untreated pristine cotton, cut into swatches of 1.5 cm² each.

2.4. Characterization of functionalized cotton loaded with ZnO NFs

The cotton fabric loaded with ZnO nanoflowers (NFs) was characterized by SEM for verification of the density of ZnO NFs on the surface of the cotton. The loading of ZnO NFs onto the surface of cotton was measured by microbalance (Sartorius AG, Goettingen, Germany).

The surface charge and conductivity of ZnO NFs @cotton were measured by Zeta potential. Surface charge in context to the potential developed at the surface of the functionalized cotton sample was measured by (Zeta sizer Nano ZS, Melvern, USA). The 3 swatches of 1.5 cm² of functionalized cotton were dipped in DI water and sonicated for 10 min before injecting into the cell. The average values of Zeta potential and surface conductivity have been reported.

2.5. Bacterial growth and evaluation of the antibacterial activity of ZnO NFs@ cotton by colony counting method

The pathogenic *E. coli* strain stored at –80 °C in glycerol were taken from the Institute of Microbiology, University of Agriculture, Faisalabad, Pakistan. The bacterial cells were sub-cultured by inoculating on MacConkey agar at 37 °C for 24 h (Fig. 1a) then the fresh bacterial culture (equal to 1.8×10^5 CFUs/mL was adjusted by measuring the optical density with a spectrophotometer) was re-suspended in tryptic soya broth and incubated at 37 °C for 24 h. After incubation, 1 ml of broth inoculum was spread on nutrient agar following the same incubation conditions, and the number of CFUs was counted by using a colony counter (Digital Colony Counter LX12CC, LABDEX UK) before treatment. Then, ZnO NFs @cotton fabric swatches of 1.5 cm² dipped in different concentration preparations (20 µg, 42 µg, 58 µg) in triplicates were exposed to UV light ($\lambda = 254$ nm) and artificial sunlight (D65) for different time intervals (Fig. 1b). Then, these swatches were placed on an agar plate swabbed with bacterial inoculum (Fig. 1c), and the plate was incubated at prior men-

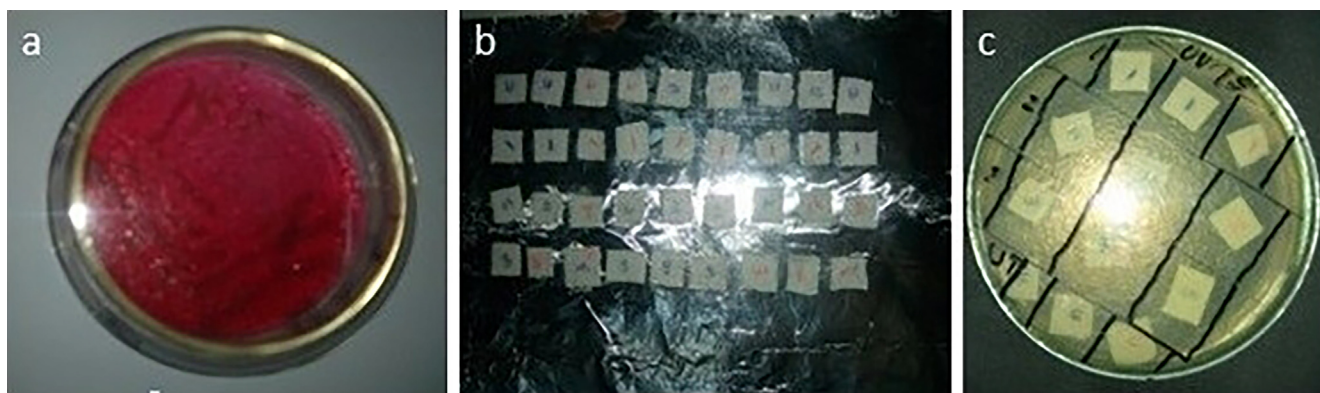


Fig. 1 (a) *E. coli* growth on MacConkey agar (b) Swatches of treated cotton fabric arranged on aluminum foil exposed to UV and artificial sunlight (c) Arrangement of irradiated swatches on agar plate.

tioned conditions and the number of CFUs was counted again with colony counter after treatment. The antibacterial activity of ZnO NFs @cotton fabric was determined by a reduction in the number of CFUs before and after treatment. However, percentage reduction (%R) was calculated by formula.

$$\text{Percent reduction (\%R)} = \frac{\text{number of colonies on untreated agar plate} - \text{number of colonies on treated agar plate}}{\text{number of colonies on untreated agar plate}} \times 100 \quad (1)$$

2.6. Determination of antibacterial activity by Breed Smear's method

Breed's smear method was used to measure the antibacterial activity of ZnO NFs by counting the number of bacterial cells in liquid broth under the microscope (Prescott and Breed 1910). Briefly, 0.1 ml of 24 h incubated fresh bacterial broth inoculum with untreated cotton swatches dipped in it was taken on the Petroff-Hausser counting chamber slide, and the number of bacterial cells was counted in small squares under a microscope. Then, ZnO NFs @cotton swatches loaded with different concentrations of ZnO NFs were dipped in different bacterial inoculated broth tubes and tubes were incubated at 37 °C for 24 h. Again, 0.1 ml of freshly incubated broth from all preparations was taken on a counting slide, and the number of bacterial cells was counted in small square fields under a microscope. Then the average number of bacterial cells was counted by formula (2), and the total number of bacterial cells per ml was counted by formula (3). The antibacterial activity was evaluated by the difference in the number of bacterial cells of treated and untreated samples.

$$\begin{aligned} \text{Average number of bacterial cells per square} \\ = \frac{\text{Total bacterial cells counted small squares}}{\text{Number of squares counted}} \end{aligned} \quad (2)$$

$$\begin{aligned} \text{Number of bacterial cells per ml} \\ = \text{Average number of bacterial cells per square} \\ \times \frac{1}{\text{square volume}} \times \text{dilution} \end{aligned} \quad (3)$$

2.7. Evaluation of antibacterial activity of ZnO NFs by MIC and MBC determination

The MIC and MBC of ZnO ZnO NFs were determined by microdilution assay. Briefly, 50 µL of each bacterial inoculum

and nutrient broth was added from well 1st to 11th in the micro titration well plate while keeping the 12th well as a negative control containing only nutrient broth. Then, serial dilutions of ZnO NFs were made from well 1st to the 10th well starting from 5000 mg/L to 9.76 mg/L while keeping the 11th well as a positive control containing only bacterial inoculum and nutrient broth. Then the plate was incubated at 37 °C for 24 h. The MIC and MBC were calculated by measuring the difference in the optical density of the plate before and after incubation by spectrophotometer (BioTek Epoch Microplate Spectrophotometer, USA) at 600 nm.

2.8. Estimation of hydroxyl radical ($\bullet\text{OH}$) generated by ZnO NFs @cotton

Hydroxyl radicals were estimated using time-resolved PL spectroscopy. Terephthalic acid (TA) with hydroxyl radicals forms a 2-hydroxyl terephthalic acid complex which gives fluorescence and its intensity is a direct measure of hydroxyl radical concentration (Vijayaraghavan 2017). In a typical procedure, to 100 ml aqueous medium containing 1.5 cm² swatch of ZnO NFs @cotton, 2 mM of TA was added and irradiated under UV light for 0–45 min. At regular intervals of 2.5 min, 2 ml aliquots were withdrawn and fluorescence was measured at an excitation wavelength of 240 nm. The same procedure was adopted for the determination of OH• radical concentration upon artificial sunlight irradiation in the time duration of 0–180 min. The aliquot of 2 ml was taken out every 20 min. The intensity of emission at 427.5 nm was correlated to the hydroxyl radical concentration produced upon irradiation.

2.9. Reusability and durability of ZnO NFs @cotton for antibacterial activity

The nano-finished cotton swatches loaded with 58 μg were washed in laundrometer (TC-M-25) 20 times and after every 5 washes, the antibacterial activity was investigated using the same procedure.

3. Results and discussion

The photocatalytic efficiency (PCA) of nanometal oxides varies based on the following factors such as crystalline structure, morphology, surface composition, surface defects, and surface charge. The role of all factors mentioned above, affecting the PCA of ZnO has been investigated. Generally, the enhancement in PCA is related to the aspect ratio, specific surface area, and charge of nanostructures, which is directly related to the precursors and method of synthesis (Zhang et al., 2014).

3.1. Structural aspects of ZnO NFs

3.1.1. Morphology of ZnO NFs @cotton

SEM micrographs of nano ZnO powder prepared by the precipitation method have been obtained and explained in a previous article (Ashar et al., 2016). The jasmine flower-like morphology was tailored owing to the self-assembly and secondary growth of stunted petal-like rods of ZnO, which occurred after primary growth. The specific 3D micro/nanostructure was highly crystalline as delineated by XRD. The crystalline properties have already been reported in a previous article (Ashar et al., 2016).

The cotton fabric loaded with ZnO NFs and binder was examined for the verification of dense covering of cotton with ZnO NFs (Fig. 2a, b). The micrographs have indicated the thorough covering of ZnO NFs onto the strands of cotton. The binder molecules were also found on the surface of cotton strands. The shape of intact nanoflower was not visible due to sonication carried out for the dispersion of ZnO NFs in water. In addition to the surface-adhered binder, the detached laminas of petals with tapered ends can be seen in the micrographs.

In our previous study, the crystalline nanoflowers of ZnO were obtained following the precipitation method. The self-assembly of nanoclusters led to the minimization of energy leading to oriented agglomeration. Moreover, the stunted rod-like nanostructures with tapered ends bearing crystalline defects gathered around the core. Conclusively, the reconstructed structures become thermodynamically stable by interconnections of nanorods in all potential directions. The mechanism involved in tailoring nanoflowers is consistent with the literature (Liang 2012, Zhou et al., 2015). The tailoring of nanostructures involved the fabrication of specific morphology happening in three stages i.e. firstly nanoclusters are formed when precursors react, and they get oriented for further attachment involving nucleation and growth (Zhang et al., 2012). The nanoclusters generated during the primary growth possessed high Gibbs free energy rendering them unstable. The Ostwald ripening is considered as a basic reason causing the secondary growth of nanoparticles to attain thermodynamic stability (Sun et al., 2012).

The bacteriostatic and bactericidal processes involve both chemical as well as physical changes. If the size of ZnO is very small like in our case, the surface area increases substantially to get a greater number of bacteria in contact. Moreover, the laminas of nanoflowers were highly polar and positively charged due to the presence of an excess of Zn^{+2} at the surface, which can attract the negatively charged cell wall of *E. coli*. The invagination and internalization of ZnO NFs and Zn^{+2} lead to the disintegration of the permeability barrier and malfunctioning of the cellular organelles causing growth inhibition. This fact can be attributed to the release of Zn^{+2} ions in the bacterial culture adhering to the cell wall modifying its membrane structure and finally its mortality (Ijaz et al., 2017, Jiang et al., 2020, Bhutta et al., 2021).

3.1.2. Internal structural aspects of ZnO NFs

TEM of ZnO NFs was obtained after sonicating the suspension of ZnO NFs in DI water. The micrographs indicated that nanoflowers were made up of stunted rods with tapered pointed ends. A few jasmine flowers can be seen in the micrograph, which remained intact even after sonication with six petals and a bud in the center (Fig. 3a). The average length of each rod (petal) was 120 nm while the average width of

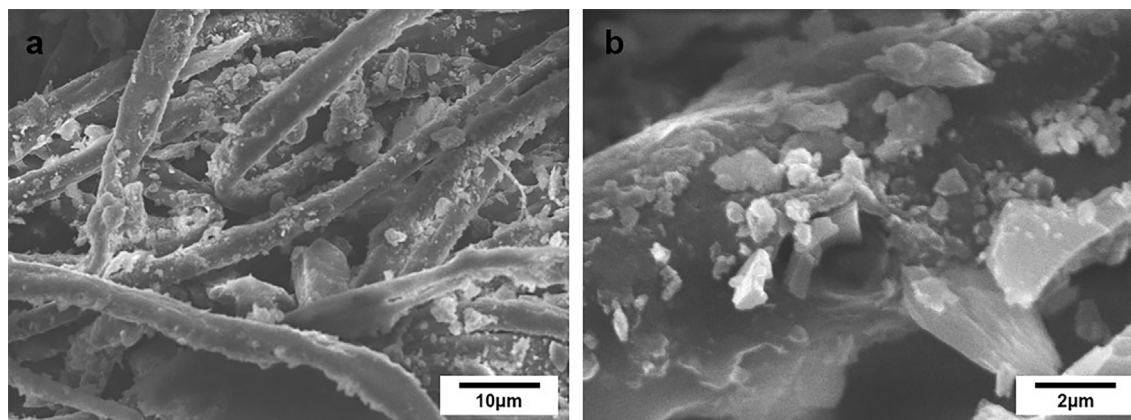


Fig. 2 SEM of cotton coated with ZnO NF (a) strands of cotton fabric covered densely with ZnO NF 5KX (b) Single strand of cotton with a dense covering of ZnO NF and binder 20 KX.

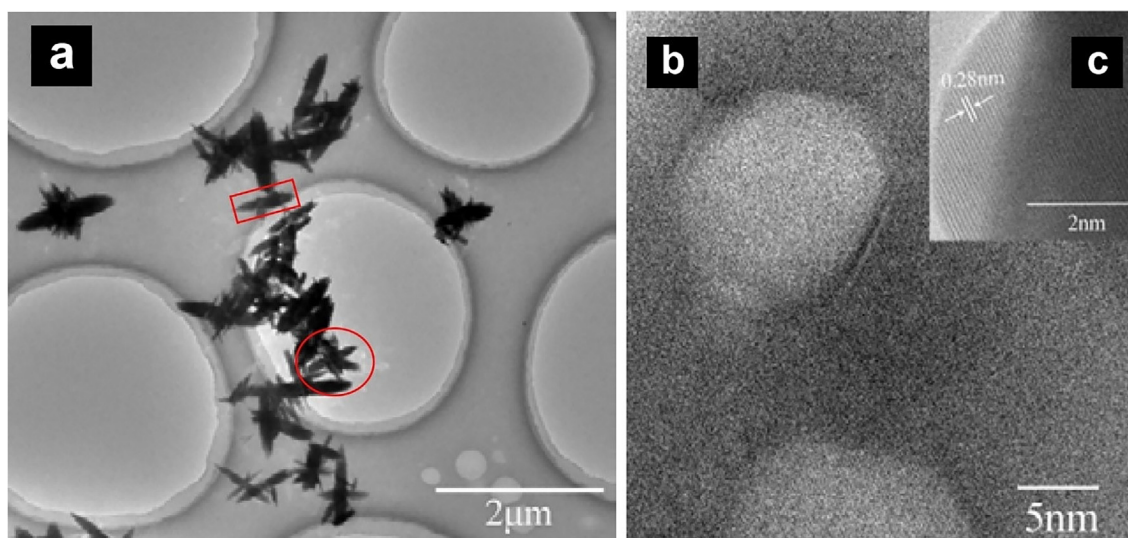


Fig. 3 (a) TEM of ZnO NFs indicating the jasmine flower-like structure (b) HRTEM of ZnO NFs exhibiting monocrystalline nature of petals of flowers with high crystallinity (c) HRTEM for d-spacing of ZnO NFs.

the rod was 23 nm as measured by image-j software, while the average size of the whole flower was 255 nm (Fig. 3a). The tapered ends and flat laminas of ZnO NFs contained numerous active sites to attract *E.coli*. Furthermore, the pointed ends of needle-like stunted rods were very appropriate in shape to pierce and penetrate the cell wall of gram-negative bacteria, made up of a compact Lipopolysaccharide layer.

Nanorods have a higher aspect ratio with a superior fraction of unsaturated Zn^{2+} sites meaning more defects due to oxygen vacancies (Zhang et al., 2014). The HRTEM of nanorods obtained from ZnO NFs has delineated the refined monocrystalline structure with a spacing of 0.28 nm (Fig. 3 b, c). The parallel lines of very low d-spacing confirmed the monocrystalline structure of ZnO NFs, suggesting the high prospects of a generation of charge carriers. Moreover, studies have suggested that rod-shaped nanostructures are safer demonstrating higher uptake by bacterial cells as compared to other morphologies (Liew et al., 2022). It has also been confirmed by other researchers that highly crystalline nanostruc-

tures can exhibit remarkable bactericidal activity (Perelshtein et al., 2015).

3.1.3. Surface elemental composition of ZnO NFs

The elemental composition of ZnO NFs was verified by surface transmission electron microscopy (STEM) and energy dispersive electron microscopy (EDX). In the electronic image obtained from the electron beam, the reshaped nanoflowers can be seen. The spotted images in red and green color delineated that excess oxygen was present at the surface in comparison to zinc. Fig. 4 a, b, c indicated the creation of oxygen deficiencies and the presence of anti-site non-coordinated Zn^{2+} ions. This condition was helpful in the creation of intrinsic defects causing an imbalance in electronic structure rendering charge transfer of carriers easier. The higher atomic % of oxygen is due to the chemisorbed oxygen at the surface, a favorable condition for photocatalytic antibacterial reaction enhancing the number of active sites (Singh et al., 2019).

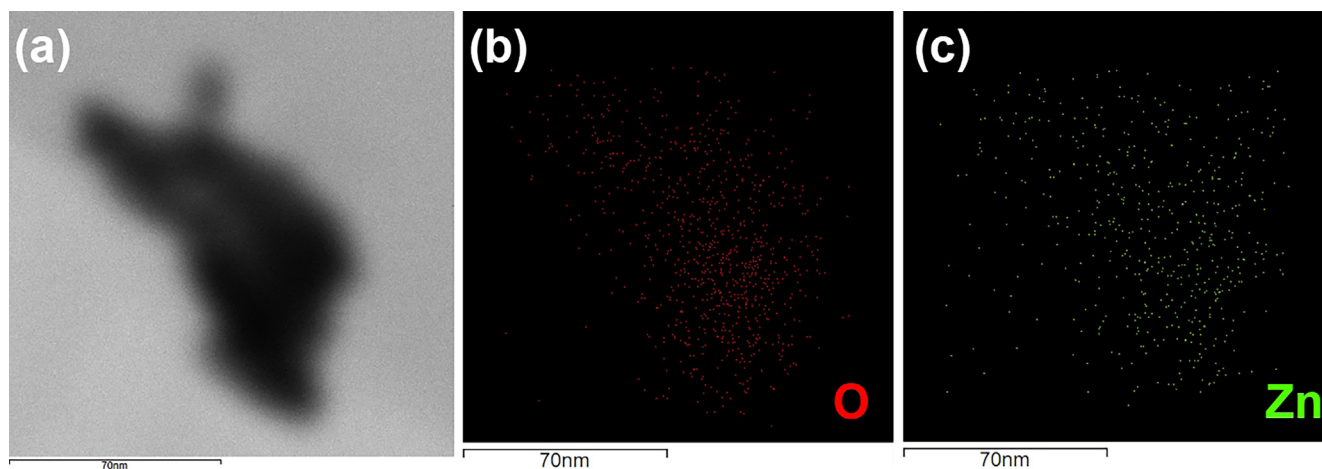


Fig. 4 (a) Electronic image of ZnO NF (b) surface concentration of oxygen (c) surface concentration of Zn.

A qualitative explanation of the importance of polar planes of ZnO NFs, stabilized by surface-bound -OH groups are subject to forming oxygen vacancies by removing either -OH groups or H₂O from the surface. Consequently, the ZnO samples with greater areas of polar planes, generally contain more oxygen vacancies. According to previous results, more oxygen vacancies in the crystal lattice can be attributed to the secondary growth of the nanostructures (Li et al., 2008).

3.1.4. Thickness of nano laminas and surface roughness of ZnO NFs by AFM

The thickness of ZnO NFs was further investigated through AFM. The tapping mode of AFM indicated the thickness of nano flowers and the roughness of the surface (Fig. 5). Maximum thickness of the discs has been found 20.1 nm while the minimum thickness was 3.4 nm according to the tapping mode scale of cantilever. The depth histogram has also delineated the average thickness of nano laminas of petals as 7 nm. The thin crystalline structures of nano laminas caused the acceleration in the transportation of charge carriers resulting in increased ROS generation required for the mortification of *E. Coli* (He et al., 2014). The deep and shallow ridges appearing on the surface of flowers can be seen below indicating the roughness of a surface. The results were found concurrent with TEM results,

showing the surface of nanoflowers bearing valleys of varied depth. The roughness of the petals of nanoflowers is favorable to attracting and capturing *E.coli* due to compatible size and charge on the cell wall. The increases in the roughness of the surface enhance the area-to-mass ratio which promotes the adsorption of bacterial proteins onto the surface of nanoparticles (Ben-Sasson et al., 2014).

3.2. Surface charge of ZnO NFs

The confirmation of surface polarity and surface charge of ZnO NFs @cotton was executed by zeta potential measurement to be assured about the presence of coulombic forces generated due to the generation and surface transportation of charge carriers. As illustrated in the graph of zeta potential (Fig. 6), the positive potential range predicted the enhanced rate of attraction of *E. coli* towards the surface of ZnO NFs. The average value of the zeta potential measured was 22.7 (mV), while the conductivity was 2.60 (mS/cm). these values conferred that the number of charge carriers at the surface of ZnO NF was appreciably high.

Similar results have been reported considering that electrostatic attraction developing between positively charged nanoparticles and the cell wall of bacteria renders them prone

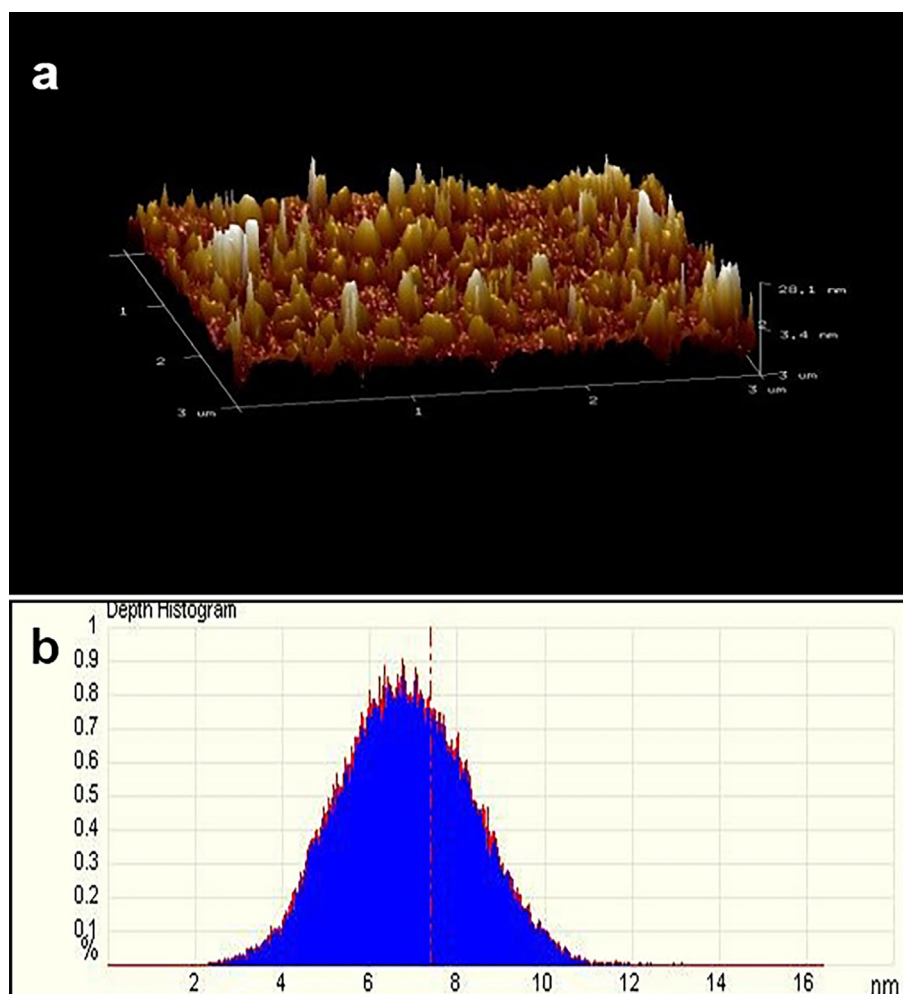


Fig. 5 (a) Tapping mode of AFM indicating the surface roughness and thickness of ZnO NFs (b) Depth histogram of ZnO NFs.

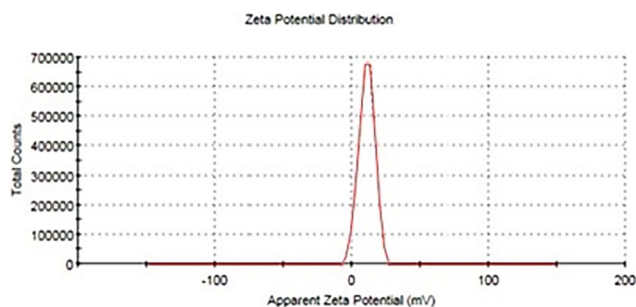


Fig. 6 Zeta potential distribution of ZnO NFs for surface charge estimation.

to adsorption onto the bacterial cell wall. Contrarily the negatively charged particles can adsorb less effectively, so the high positive potential of NPs helps in gathering at the sites of bacterial infection (Fang et al., 2015). The greater concentrations of positively charged nanoparticles have been reported to exhibit a high level of antibacterial efficiency because of their convenient crowding onto the bacterial surface (Arakha et al., 2015). It has been reported that illumination increases the anti-bacterial performance of ZnO nanoparticles as compared to the action of unilluminated nanostructures (Li et al., 2007).

3.3. Optical properties of ZnO NFs and ZnO NFs@Cotton

The diffused reflectance spectroscopy (DRS) has revealed the optical properties of ZnO NFs and ZnO NFs@cotton in terms of the extent of UV and visible radiations harvested by nanoflowers. The % reflectance has shown that ZnO NFs can absorb 40% of sunlight while 90% of UV radiations below 380 nm. Furthermore, ZnO NFs@cotton has a 32% harvesting capacity for sunlight and 90% of UV radiations (Fig. 7 a). This is the reason that the nanoflowers exhibited accelerated and magnificent antibacterial activity on illuminating them with ionizing UV radiations. The bandgap energy of ZnO NFs by using has been determined by using the Kubelka-Munk method using the data obtained by DRS (Ashar et al., 2020). The value of bandgap calculated for ZnO NFs was 2.95 eV, while 2.98 eV for ZnO NFs@cotton, confirming the capability of both to harvest solar radiations in addition to UV radiations (Fig. 7b). The bend appearing in the curve delineated the presence of surface defects present in ZnO NFs. The other important factor regarding antibacterial activity is the presence of morphology-dependent surface defects such as oxygen vacancies (Xu et al., 2013). The oxygen vacancies are considered charge trap centers induced upon irradiation which not only act as active sites but also decrease the bandgap of ZnO.

Although doping of ZnO using metals and non-metals is considered a prevailing and fruitful procedure to decrease the band gap of nano ZnO, but generation of intrinsic point defects can successfully develop suitable electrical and optical properties (Tang et al., 2017). According to previous studies manipulation of crystal lattice by creation of native point defects termed defect engineering, is an easier yet effective approach to enhancing PCA of ZnO (Masar et al., 2023). To extend the light-harvesting tendency of ZnO in the visible region of sunlight bandgap reduction is required, which can

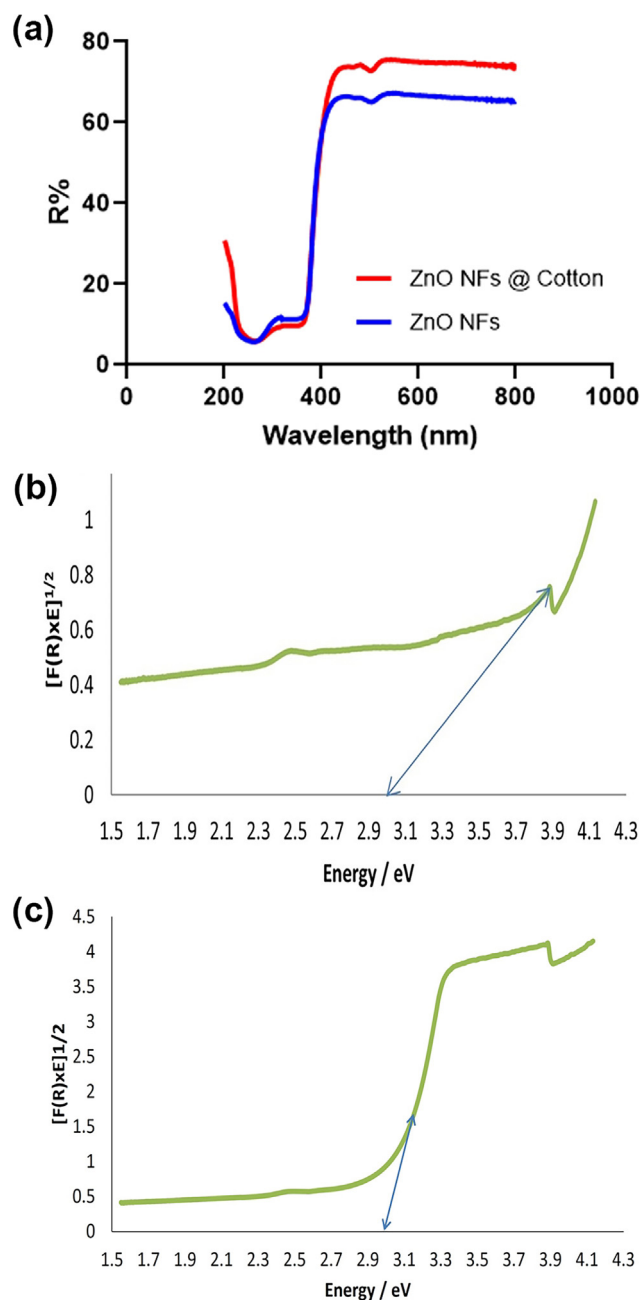


Fig. 7 (a) Diffused reflectance spectroscopy of ZnO NFs and ZnO NFs @ cotton (b) Bandgap energy of ZnO NFs obtained by plotting the results of DRS (C) Bandgap energy of ZnO NFs @ cotton obtained by plotting the results of DRS.

be achieved by induction of native defects in ZnO (Eixenberger et al., 2019).

A Study has revealed that even in the absence of light aqueous suspension of ZnO oxygen vacancies found in the crystal lattice facilitate the ROS generation (Lakshmi Prasanna and Vijayaraghavan 2015). Among all native crystal defects of ZnO, oxygen vacancies are examined to exhibit higher benefits regarding substantial enhancement in intrinsic properties of ZnO for numerous applications (Wang et al., 2018). It is proved in previous reports that H_2O_2 is generated in the aqueous suspensions of ZnO in the dark as well as causing oxidative

stress in bacteria resulting in antibacterial activity (Xu et al., 2013). The crystal defects can mediate ROS generation in the dark, but absorption of visible and UV radiations enhances the excitation of charge carriers. Production of higher amounts of ROS upon irradiation, results in highly substantial antibacterial activity than that obtained in the dark (Applerot et al., 2009).

3.4. Oxygen vacancies in ZnO NFs

Photoluminescence spectroscopy can provide important insight into crystal characteristics such as surface defects, oxygen vacancies, photoinduction of charge carriers, their movement, and recombination involved in semiconductor nanostructures. According to Fig. 8a, the excitation spectrum of ZnO NFs exhibited a narrow but high luminescence band at 320 nm while a broad and short band occurred at 380 nm. The bands appearing delineated the capability of harvesting both UV and visible radiations. The most prominent band that appeared in the emission spectrum of ZnO NFs was at 425 nm in addition to a small peak appearing at 315 nm and a broader one at 400 nm (Fig. 8 b). The small peaks in the UV region indicated a very low rate of recombination of charge carriers. Generally, ZnO nanostructures of different morphology like nanorods(1D) or nanoparticles (0D) exhibit one or two narrow luminescence peaks appearing in the UV region termed as near band emission (NBE) and a broad band in the visible region of the spectrum called as deep level emission (DLE). Examining the PL band position and intensity and the ratio of NBE/ DLE, the structural features of ZnO nanostructures can be investigated. The DLE is linked to ZnO defects, such as zinc vacancies, ionic oxygen vacancies, neutral oxygen vacancies, and oxygen interstitials. The enhanced PCA in the visible spectrum has been attributed by the scientific community to oxygen vacancies causing the induction of band-gap narrowing (Wang et al., 2012). According to previous reports, the increase in the density of oxygen vacancies in the crystal lattice of ZnO leads to the enhanced antibacterial activity of nanoparticles (Wang et al., 2017).

The high concentration of OH• generated during photocatalysis has been determined through a PL study. This may be correlated to exposure of (001) highly charged polar facets of ZnO NFs laminas to *E. coli* possessing its ability to exhibit

magnificent PCA regarding bactericidal action. This enhancement in PCA can be attributed to a higher number of active sites available on a polar facet (Ramirez-Canon et al., 2018). Previously it has been explained that the antibacterial activity of ZnO not only depends upon the aspect ratio and crystallite size but another prominent factor is oxygen vacancies present on the surface of nanostructures. The broadband in the visible-light region is widely considered to result from ZnO surface defects, in which oxygen vacancies are the most suggested defects. The highly polar morphology caused a marked increase in the intensity of the emission band in the visible region commonly endorsed to intrinsic defects such as oxygen vacancies (Farha et al., 2020). Herein, the occurrence of this deficiency advocates an excess of Zn²⁺ ions onto the highly polar surface of ZnO nanostructures concluding the potential correlation between oxygen vacancy and polar planes of ZnO (Johnson et al., 2022).

3.5. Concentration of OH• radicals generated by ZnO NFs

The swatch of 1.5 cm² ZnO NFs@ cotton loaded with 42 µg of the photocatalyst was dipped in 50 ml solution of 0.004 mM of terephthalic acid was irradiated with UV light for 0–45 min and artificial sunlight for 0 to 180 min. On excitation of irradiated suspension, the peak of hydroxy- terephthalic acid appeared at 425 nm and the extent of rise of the peak indicated the concentration of OH• generated in 180 min. The results of the blank experiment indicated that a low signal was generated at 427.5 nm in the absence of a catalyst. It can be seen that 42 µg of ZnO NF has shown a peak up to 495 a. u. upon UV irradiation and up to 380 a. u. upon artificial sunlight irradiation. The peaks obtained indicated that a much higher OH• concentration was produced by ZnO NFs @cotton by UV irradiation in 45 min as compared to the sunlight exposure of 180 min (Fig. 9 a, b).

The previous researches also explain that ZnO produces minimum amounts of OH• in the dark as the main antimicrobial moiety which increases magnificently when it is stimulated using radiation sources. The number of oxygen vacancies that are located on the surface of ZnO as a heterogeneous photocatalyst plays a remarkable role in the production of H₂O₂. Furthermore, the photocatalytic activity of metal oxides in

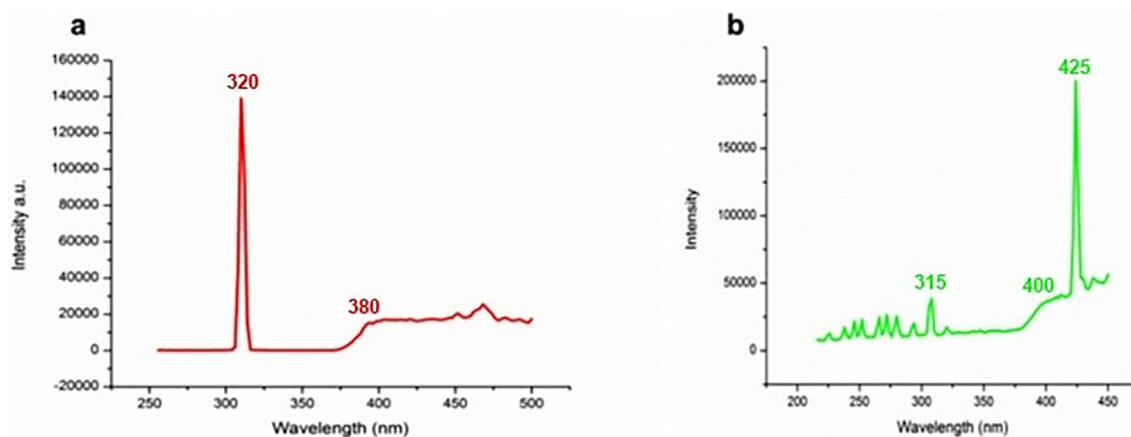


Fig. 8 Room temperature PL spectra of ZnO NFs a) Excitation spectrum b) Emission spectrum.

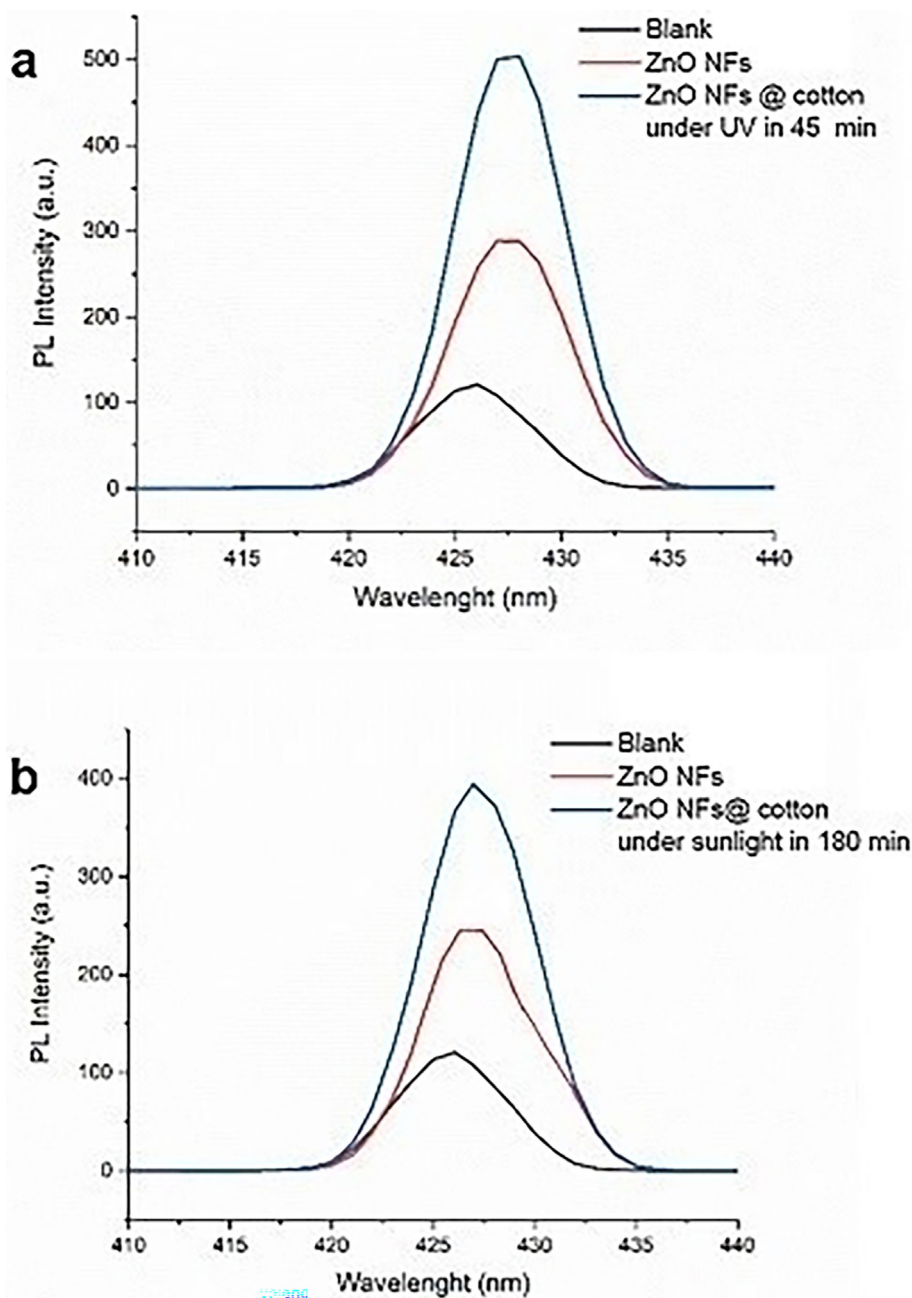


Fig. 9 Determination of $\text{OH}\bullet$ radical generation by ZnO NF using room temperature time-resolved PL.

the context of the mortification of bacteria is governed by the density of active sites.

Since $\text{OH}\bullet$, produced by ZnO and H_2O_2 , is a highly reactive moiety possessing a diffusion-limited capability to react (Iuga et al., 2011); hence it can only employ its action on neighboring structures or cells. It can be hypothesized that enhancement of the adsorption of nanostructures onto the bacterial cell wall results in higher concentrations of $\text{OH}\bullet$ being generated in the locale of bacteria exhibiting higher antibacterial activity (Alkawareek et al., 2019). The ROS has been investigated as a major parameter that can lead to intracellular outflow of cytoplasmic contents, mitochondrial damage, and oxidative stress finally causing inhibition of bacterial cell growth leading

to death. Conclusively, the production of H_2O_2 is considered as a crucial motive for the bactericidal activity of ZnO (Liu et al., 2019). The defect-rich surface of ZnO can be obtained by the methods showing kinetically controlled reaction conditions to obtain higher ROS concentration (Liu et al., 2019).

3.6. Antibacterial activity of ZnO NFs@ cotton

3.6.1. Antibacterial activity of cotton fabricated ZnONFs

The different preparations of cotton-fabricated ZnO NFs were tested for antibacterial activity at different exposure times to UV and sunlight by colony counting (CFUs/mL) and cell

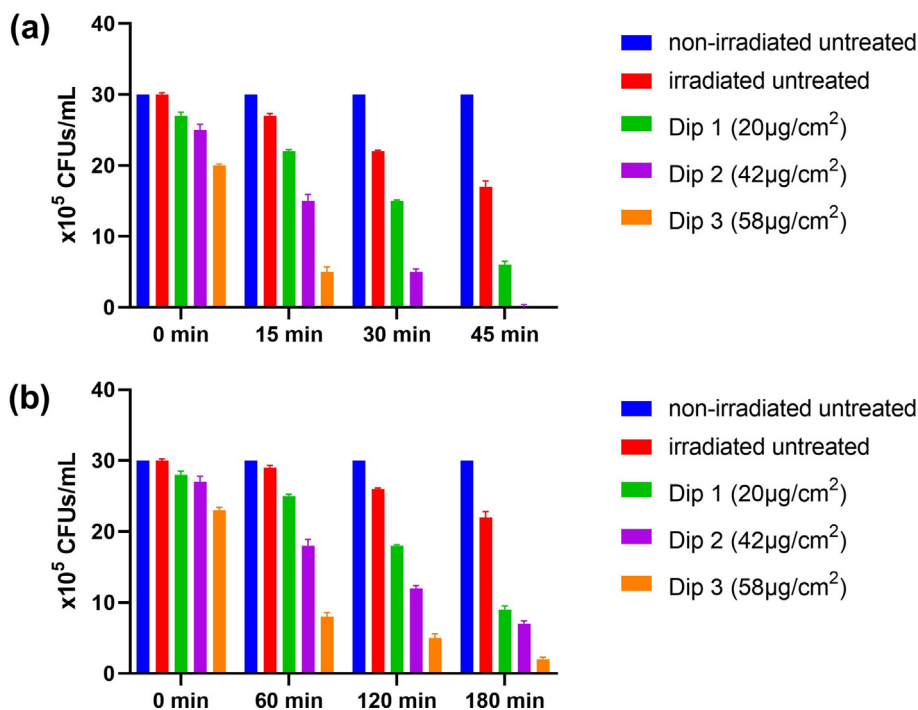


Fig. 10 Antibacterial efficacy in terms of CFUs/mL of ZnO NFs @cotton after irradiation to (A) UV light and (B) Sunlight for different time intervals.

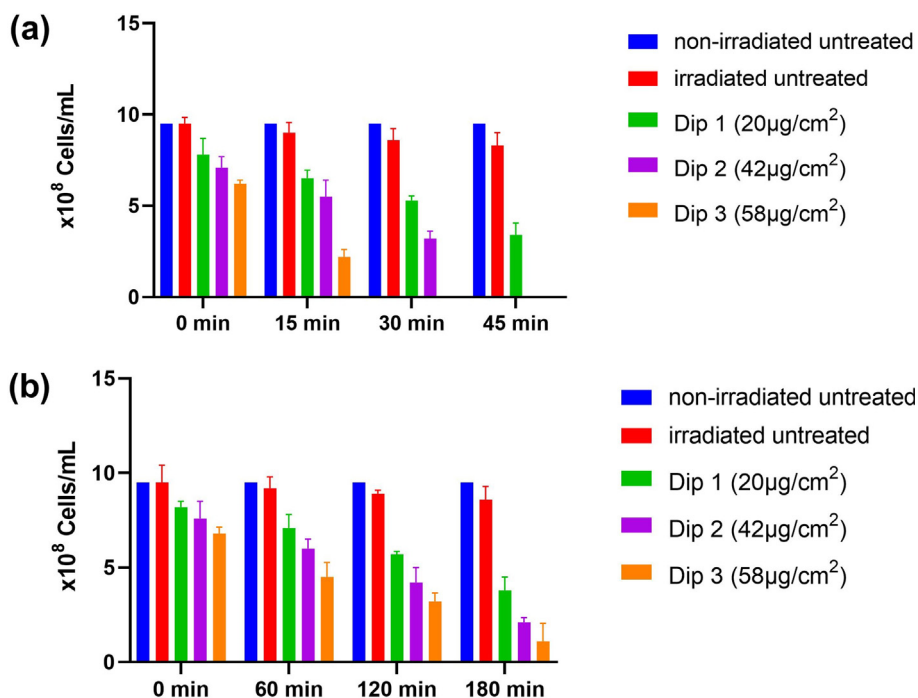


Fig. 11 Antibacterial activity in terms of bacterial cells/mL of different concentrations of ZnO NFs @cotton swatches after irradiation to UV and sunlight for various time intervals.

counting (cells/mL) methods. The overall study findings revealed that short-time irradiation of ZnO NFs to ionizing UV light showed higher antibacterial efficacy (fewer CFUs/mL and cells/mL respectively) as compared to longer irradiation by sunlight (Figs. 10 and 11) which is consistent with a

previous study by Ravikumar et al., (2021) who reported higher antimicrobial activity of Ag-TiO₂@Pd/C nanocomposites under UV light as compared to sunlight. The untreated cotton swatches not exposed to UV and sunlight showed no decrease in CFUs and bacterial cells. However, when the

untreated swatches were exposed to UV and sunlight at various time intervals, just a minute decrease in CFUs and bacterial cells was noted which is indicating the antibacterial activity of UV and sunlight. Moreover, ZnO NFs @cotton swatches loaded with 20 μg showed less antibacterial activity as compared to 42 μg and 58 μg loadings at all-time intervals (Figs. 10 and 11) which is consistent with the findings of Babayevska et al., (2022) who reported that increasing concentration of ZnO nanomaterials resulted in higher antibacterial activity in terms of decreased bacterial number as observed in the present study. It was also noted that an increase in irradiation time of ZnO NFs @ cotton either to UV or sunlight resulted in higher antibacterial activity at all loading levels. ZnO NFs@ cotton swatches loaded with any concentration at any exposure time interval resulted in greater percent reduction (%R) in CFUs/mL after exposure to UV light as compared to sunlight (Table 1) which is consistent with previous findings of de Lucas-Gil et al., (2018) who evaluated the antibacterial activity of ZnO nanoparticles by %R and CFUs/mL against *E. coli* and noted higher %R and lower CFUs/mL. The present study observed that sunlight irradiation of ZnO NFs@ cotton also resulted in a remarkable antibacterial activity but was slightly lower than UV irradiation. This fact can be attributed to the higher ionizing power of UV light (Taghipour 2004). The sunlight harvesting capacity of ZnO NFs was increased due to a decrease in bandgap energy and generation of ROS due to irradiating ZnO NFs@ cotton for a longer period (Bokare et al., 2013, Li et al., 2017).

3.6.2. MIC and MBC of ZnO NFs exposed to UV and sunlight

The MIC and MBC of ZnO NFs were determined by the Broth microdilution method. The experiment was performed by making two-fold serial dilutions of ZnO NFs from 5000 mg/mL to 9.76 mg/mL. Then, MIC and MBC were calculated by noting OD value before and after incubation at 600 nm by spectrophotometer. The study noted slightly lower MIC and MBC of samples exposed to UV light as compared to sunlight (Fig. 12). The MIC and MBC of ZnO NFs s exposed to UV light was noted to be 19.53 mg/mL and 39.06 mg/L respectively as compared to MIC and MBC of ZnO NFs exposed to sunlight were noted 39.06 mg/mL and 156.25 mg/mL respectively. A similar study conducted by de Lucas-Gil et al., (2018) noted approximately 5.4 mg/mL under UV which is lower than the MIC of the current study. Another study conducted by Kadiyala et al., (2018) noted 1562 mg/mL under UV which is too higher than the current findings. The differences may be due to different preparation protocols, sizes, shapes, and antimicrobial evaluation procedures (Ali et al., 2020, Babayevska et al., 2022).

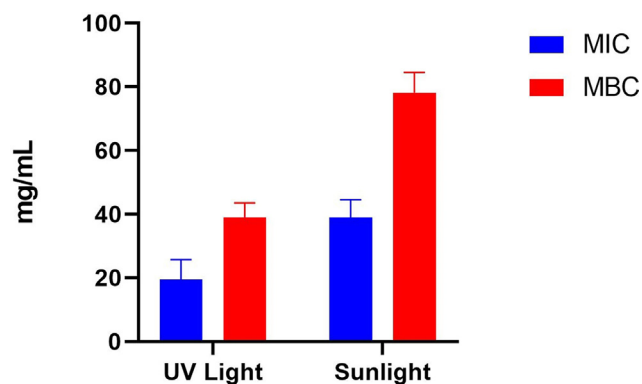


Fig. 12 MIC and MBC of ZnO NFs irradiated by UV and sunlight.

3.6.3. Mechanism of antibacterial activity

The antibacterial effect of direct contact with nanoparticles of appropriate dimensions with bacteria results because of the generation of ROS (Van Houdt and Michiels 2005, Zhang 2008). The equilibrium between the generation and degradation of ROS is disturbed due to their amplification in the cytoplasm of a cell, termed oxidative stress (Wang et al., 2017). The tailored nanoparticles have shown enhancement in oxidative stress in bacterial cells by ROS generation at or nearby their surface (Kumar et al., 2011). The rate of production of ROS increases with the irradiation of cotton fabric doped with ZnO NFs because of the high light harvesting ability, low bandgap, and increased surface area (Ashar et al., 2021). Due to the increased absorption of sunlight and UV light by ZnO nanoflowers doped on cotton fabric results in the excitation of electrons (e^-) and produces more hydroxyl radicals (OH^\cdot) which can react with O_2 in the environment as revealed by STEM, high level of oxygen atoms presents on the surface of ZnONFs resulted in high bactericidal efficiency of ZnO NFs@cotton (Fig. 13) and reaction with oxygen produce more strong superoxide radicals (O_2^\cdot), and destroy the cellular components such as chromosomal DNA, protein denaturation, and physical disruption of cellular membranes and ultimately lead to cell death due to oxidative stress, production of ROS, and holes formation in membrane (Dastjerdi and Montazer 2010, Rahmat et al., 2021). These charge carriers can migrate up to the outermost ZnO surface to react with the aqueous external environment, resulting in the generation of ROS (Song et al., 2010). The thickness of nanostructures also plays an important role in their migration. Moreover,

Table 1 Antibacterial activity of ZnO NFs @Cotton in terms of % reduction in CFUs/mL.

% Reduction in CFUs/mL after exposure to UV light					% Reduction in CFUs/mL after exposure to sunlight				
Exposure Time	Irradiated untreated	20 μg	42 μg	58 μg	Exposure time	Exposed untreated	20 μg	42 μg	58 μg
0 min	0.00%	10.0%	16.6%	33.3%	0 min	0.00%	6.66%	10.0%	23.3%
15 min	10.0%	26.6%	50.0%	83.3%	60 min	3.33%	16.6%	40.0%	73.3%
30 min	26.6%	50.0%	83.3%	100%	120 min	13.3%	40.0%	60.0%	83.3%
45 min	43.3%	80.0%	100%	100%	180 min	26.6%	70.0%	76.6%	93.3%

Antimicrobial Activity Mechanisms

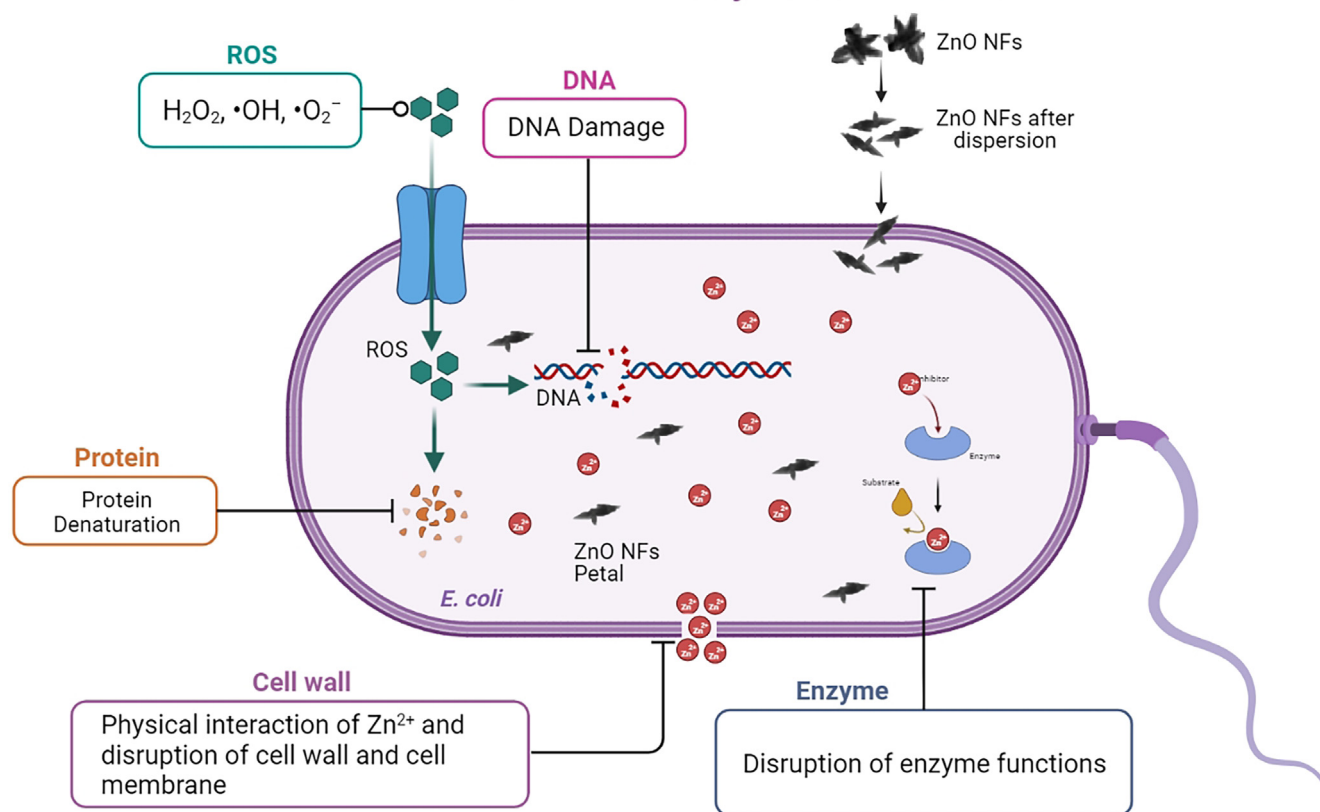


Fig. 13 Proposed antibacterial activity of ZnO NFs.

the band-gap engineering of ZnO is also a valuable tool to increase the number of charge carriers to magnify the efficiency of this process. The reduction in the energy required to generate free electrons and controlling the efficiency in ROS generation ultimately increase antibacterial activity (Pasquet et al., 2014).

3.6.4. Factors affecting the antibacterial activity

The antibacterial activity of ZnO NFs@ cotton against gram-negative bacteria can be attributed to the production of H_2O_2 , capable of readily generating ROS with higher potential. The effect of ZnO NFs took place in a pH range between 5 and 7, and upon its dissolution, Zn^{2+} as a product contributed to the antibacterial activity (Gross and Kornijów 2002, Wolanov et al., 2013). It has been observed that metal ions when sluggishly released from nano-scaled metal oxide, penetrate the cell membrane on interaction with the proteins. The functional groups of proteins such as carboxyl groups, mercapto, and amino are denatured, damaging the cell membrane and enzyme activity. Furthermore, alterations in the cell structure, inhibiting the normal physiological functions ultimately mortify *E. coli* (Aung et al., 2016).

3.6.4.1. Morphology of antibacterial nanoparticles. Regarding antimicrobial activity, a huge challenge is designing nanoparticles with suitable aspect ratio, surface area, and morphology, which can be modified and tuned. The morphology i.e. shape, surface roughness, and thickness of nanoparticles affect their

biological actions like cell internalization. Thus, morphology along with surface area influences the antibacterial activity, and it is essential to fabricate nanostructures with appropriate morphology, bearing a high density of adsorption sites based on a large surface area (Singh et al., 2019). The verification of morphological aspects of the nanomaterials especially the specific surface area shows magnificent potential for their bio-applications (Babayevska et al., 2022).

Previous researches have explained that hierarchical morphology exhibits remarkably good antimicrobial activity among various other morphological versions. Allegedly, the significantly large surface area of nanoparticles enhances bactericidal activity by permitting higher surface contact with bacteria. The penetration of the bacterial cell wall and disorganization of the cell membrane upon surface contact with ZnO NFs have been indicated to inhibit bacterial growth (Zille et al., 2014).

The solution phase synthesis of nanoparticles involves processes like Ostwald ripening and epitaxial connection related to competition between the rate of nucleation and growth to modify the particle size and shape. Initially, the mixing of precursors leads to nucleation, followed by the growth of nanoparticles until the super-saturation dwindles. Furthermore, the high rate of growth as compared to nucleation cause coarsening and aggregation of particles. Studies show that aggregation into 3D morphology depends on the surface chemistry of the particles resulting in random arrangement or oriented attachments of 1D or 2D nanoparticles. Addition-

ally, the creation of porous clusters of nanoparticles occurs due to their random aggregation, while epitaxial attachment of nanoparticles leads to the fabrication of secondary growth of particles with novel morphologies (Sun et al., 2006).

In our study, the nucleation of ZnO occurred through precipitation, involving the slow reaction between metal salt with hydroxide ions. The growth of stunted and pointed rod-like 1D structures was under gone coarsening, which involved tailoring of larger crystals that expanded to adapt petal like shape and joined to look like a jasmine flower upon oriented aggregation. The chemical potential of a nanoparticle has already been confirmed to increase with decreasing particle size (Chen et al., 2014).

3.6.4.2. Release of Zn^{+2} ion in the cytoplasm of bacteria. The major factor proposed for the antibacterial mechanisms for ZnO NFs is the release of Zn^{+2} ions in an aqueous medium containing ZnO NFs and *E. coli* based on the dissolution behavior. ZnO has a tendency to get slowly dissolved in water producing free Zn^{2+} ions. The dissolution tends to occur more easily in the presence of a large surface area of nanoparticles owing to boosted surface reactivity (Sirelkhatim et al., 2015). In previous reports, Zn^{2+} ions have been extensively and successfully investigated for intensification of the antibacterial activity of ZnO (Li et al., 2011).

The released Zn^{+2} ions have a significant role in the inhibition of active transportation through the cell membrane, disruption of enzymatic systems in addition to disturbance in the metabolism of proteins. However, the engineered nanostructures exhibit modification in their bactericidal activity by controlling the rate of dissolution based on surface composition and morphology. In our study, supposedly, the laminated morphology and small size of rods enhanced the rate of release of Zn^{+2} ions in the medium containing ZnO NFs @cotton. According to numerous studies, the Zn^{+2} ions released into the growth medium are responsible for size-dependent nanotoxicity and the extent of dissolution of ZnO NFs into Zn^{+2} ions (Xia et al., 2008).

3.6.4.3. ROS generation by ZnO NFs @cotton. The mechanisms involved in antibacterial activity have been attempted to be investigated using TiO_2 @ textile. The TiO_2 nanostructures were found to produce reactive oxygen species (ROS) such as superoxide radical anion, hydroxyl radicals, and a positive hole (Yang et al., 2004). These ROS are capable of interacting with the cell wall and then the cell membrane of bacteria which eventually leads to cell death. (Bozzi et al., 2005). The ROS can also decompose the oil, dirt, and organic matter hence imparting self-cleaning properties to textiles.

3.7. Durability of ZnO NFs@ cotton

The ZnO NFs @ cotton loaded with 58 μg was washed 20 times and antibacterial efficiency against *E. coli* was determined after every 5 washes. The antibacterial efficiency was observed to be maintained for 15 washes and after that, it gradually decreased. However, the total decrease in efficiency of ZnO NFs @ cotton after 20 cycles was only 5% (Fig. 14). This effect renders the nano-finished cotton reusable even after 15 washing cycles retaining its antibacterial activity against *E. coli*. Considering the previous studies Li and colleagues inves-

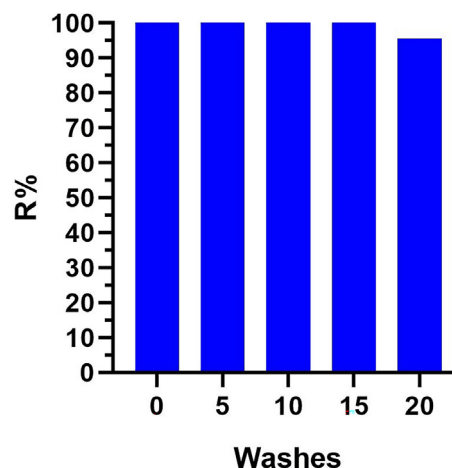


Fig. 14 The durability and reusability of ZnO NFs @ Cotton as an antibacterial agent.

tigated the durability of the antibacterial activity of functionalized cotton fabric loaded with nano-ZnO to sweat. The durability of the anti-bacterial activity of the finished cotton fabric in acidic, alkaline, and salt-based artificial sweat solutions was evaluated. The results have shown better salt and alkaline resistance than acid resistance for the treated fabrics (Li et al., 2007). In another study, Xu and Cai et al., have grown ZnO nano-rod on cotton fabric samples through the dip-pad-cure process, which exhibited washing stability (Xu and Cai 2008).

4. Conclusion

The previously synthesized powdered, ZnO NFs have been utilized to prepare functionalized cotton. The nano-finished cotton was examined to have a dense covering of positively charged ZnO NFs in the form of flowers and unassembled rod-shaped petals. The optical properties delineated the band gap energy and radiation harvesting capability of ZnO NFs under UV and artificial sunlight D65. The surface-adhered ZnO NFs exhibited a suitable bandgap of 2.9 eV to act as an active semiconductor both in UV light and visible portion of solar radiations. The high photocatalytic activity of ZnO NFs can be attributed to the presence of oxygen vacancies as crystal defects causing the magnificent ROS generation. The antibacterial activity of the fabricated samples has been determined by modified Bread's Smear method against *E. coli*. The prepared samples with different concentrations of ZnO NFs loaded onto the surface of cotton were irradiated under UV light and D65 artificial sunlight in a range of time intervals i.e. 15, 30, and 45 min and 60, 120, and 180 min respectively. The bactericidal activity was determined by a decrease in CFUs and a % reduction in the number of bacterial cells by calculating microscopic factor. The results obtained indicated that 42 μg of ZnO NFs were efficient enough to mortify 100% of *E. coli* in 30 min under UV light. While 93.3% R for 58 μg of ZnO NFs could be obtained in 45 min under D65 light. It can be concluded that upon irradiating to high energy UV light, the antibacterial activity of ZnO NFs was elevated due to a higher concentration of ROS produced as compared to artificial sunlight. Still increasing the load of ZnO NFs onto the surface of cotton, increased their efficiency regarding the mortification of *E. coli* in D65 light. The higher surface charge and greater contact area based on surface roughness accelerated the bactericidal process under UV light and artificial sunlight. The washing durability of the nano-finished ZnO NFs @ cotton was magnificent as high bactericidal activity was maintained even

after 20 washing cycles. The nano-finished cotton has exhibited high prospects to be used as a medical textile and antibacterial self-cleaning fabric.

Declaration of Competing Interest

The authors declare that they have no known competing financial interests or personal relationships that could have appeared to influence the work reported in this paper.

Acknowledgment

Princess Nourah bint Abdulrahman University Researchers Supporting Project number (PNURSP2023R153), Princess Nourah bint Abdulrahman University, Riyadh, Saudi Arabia. Also, the authors extend their appreciation to the Deanship of Scientific Research at King Khalid University, Abha, Saudi Arabia for supporting this work under the grant number (R. G.P.2/121/44). The author also acknowledges Professor Dr. Ahmed El-Shafei and Dye Chemistry and application laboratory for facilitating to conduct the part of the study.

Funding

Support of the American Association of University Women in the form of an International Fellowship award, which enabled Ambreen Ashar to attend North Carolina State University and conduct part of this study.

References

- Ahmed, H.B., El-Hawary, N.S., Emam, H.E., 2017. Self-assembled AuNPs for ingrain pigmentation of silk fabrics with antibacterial potency. *Int. J. Biol. Macromol.* 105, 720–729.
- Ali, S.G., Ansari, M.A., Alzohairy, M.A., et al, 2020. Effect of biosynthesized ZnO nanoparticles on multi-drug resistant *Pseudomonas aeruginosa*. *Antibiotics* 9, 260.
- Alkawareek, M.Y., Bahloul, A., Abulatefeh, S.R., et al, 2019. Synergistic antibacterial activity of silver nanoparticles and hydrogen peroxide. *PLoS One* 14, e0220575. <https://doi.org/10.1371/journal.pone.0220575>.
- Applerot, G., Lipovsky, A., Dror, R., et al, 2009. Enhanced antibacterial activity of nanocrystalline ZnO due to increased ROS-mediated cell injury. *Adv. Funct. Mater.* 19, 842–852.
- Arakha, M., Pal, S., Samantarai, D., et al, 2015. Antimicrobial activity of iron oxide nanoparticle upon modulation of nanoparticle-bacteria interface. *Sci. Rep.* 5, 1–12.
- Ashar, A., Iqbal, M., Bhatti, I.A., et al, 2016. Synthesis, characterization and photocatalytic activity of ZnO flower and pseudo-sphere: Nonylphenol ethoxylate degradation under UV and solar irradiation. *J. Alloy. Compd.* 678, 126–136.
- Ashar, A., Bhatti, I.A., Ashraf, M., et al, 2020. Fe³⁺ @ ZnO/polyester based solar photocatalytic membrane reactor for abatement of RB5 dye. *J. Clean. Prod.* 246, <https://doi.org/10.1016/j.jclepro.2019.119010> 119010.
- Ashar, A., Bhatti, I.A., Siddique, T., et al, 2021. Integrated hydrothermal assisted green synthesis of ZnO nano discs and their water purification efficiency together with antimicrobial activity. *J. Mater. Res. Technol.* 15, 6901–6917.
- Aung, M.S., Zi, H., Nwe, K.M., et al, 2016. Drug resistance and genetic characteristics of clinical isolates of staphylococci in Myanmar: High prevalence of PVL among methicillin-susceptible *Staphylococcus aureus* belonging to various sequence types. *New microbes and new infections.* 10, 58–65.
- Babayevska, N., Przysiecka, L., Iatsunskyi, I., et al, 2022. ZnO size and shape effect on antibacterial activity and cytotoxicity profile. *Sci. Rep.* 12, 1–13.
- Barakat, N.A., Abdelkareem, M.A., El-Newehy, M., et al, 2013. Influence of the nanofibrous morphology on the catalytic activity of NiO nanostructures: an effective impact toward methanol electrooxidation. *Nanoscale Res. Lett.* 8, 1–6.
- Benloutoufa, S., Miled, W., Trad, M., et al, 2020. Chitosan hydrogel-coated cellulosic fabric for medical end-use: Antibacterial properties, basic mechanical and comfort properties. *Carbohydr. Polym.* 227, 115352.
- Ben-Sasson, M., Zodrow, K.R., Gengqeng, Q., et al, 2014. Surface functionalization of thin-film composite membranes with copper nanoparticles for antimicrobial surface properties. *Environ. Sci. Tech.* 48, 384–393.
- Bhutta, Z.A., Ashar, A., Mahfooz, A., et al, 2021. Enhanced wound healing activity of nano ZnO and nano Curcuma longa in third-degree burn. *Appl. Nanosci.* 11, 1267–1278.
- Bokare, A., Sanap, A., Pai, M., et al, 2013. Antibacterial activities of Nd doped and Ag coated TiO₂ nanoparticles under solar light irradiation. *Colloids Surf. B Biointerfaces* 102, 273–280.
- BoopathiRaja, R., Parthibavarman, M., 2020. Reagent induced formation of NiCo₂O₄ with different morphologies with large surface area for high performance asymmetric supercapacitors. *Chem. Phys. Lett.* 755, 137809.
- Bozzi, A., Yuranova, T., Kiwi, J., 2005. Self-cleaning of wool-polyamide and polyester textiles by TiO₂-rutile modification under daylight irradiation at ambient temperature. *J. Photochem. Photobiol. A Chem.* 172, 27–34.
- Bu, Y., Zhang, S., Cai, Y., et al, 2019. Fabrication of durable antibacterial and superhydrophobic textiles via in situ synthesis of silver nanoparticle on tannic acid-coated viscose textiles. *Cellul.* 26, 2109–2122.
- Chen, Y., Zeng, D., Zhang, K., et al, 2014. Au–ZnO hybrid nanoflowers, nanomultipods and nanopyramids: one-pot reaction synthesis and photocatalytic properties. *Nanoscale* 6, 874–881.
- Creutzig, F., Agoston, P., Goldschmidt, J.C., et al, 2017. The underestimated potential of solar energy to mitigate climate change. *Nat. Energy* 2, 1–9.
- Dastjerdi, R., Montazer, M., 2010. A review on the application of inorganic nano-structured materials in the modification of textiles: focus on anti-microbial properties. *Colloids Surf. B Biointerfaces* 79, 5–18.
- de Lucas-Gil, E., Leret, P., Monte-Serrano, M., et al, 2018. ZnO nanoporous spheres with broad-spectrum antimicrobial activity by physicochemical interactions. *ACS Applied Nano Materials.* 1, 3214–3225.
- Desai, M.A., Vyas, A.N., Saratale, G.D., et al, 2019. Zinc oxide superstructures: recent synthesis approaches and application for hydrogen production via photoelectrochemical water splitting. *Int. J. Hydrogen Energy* 44, 2091–2127.
- Eixenberger, J.E., Anders, C.B., Wada, K., et al, 2019. Defect engineering of ZnO nanoparticles for bioimaging applications. *ACS Appl. Mater. Interfaces* 11, 24933–24944.
- Fang, B., Jiang, Y., Nüsslein, K., et al, 2015. Antimicrobial surfaces containing cationic nanoparticles: How immobilized, clustered, and protruding cationic charge presentation affects killing activity and kinetics. *Colloids Surf. B Biointerfaces* 125, 255–263.
- Farha, A.H., Al Naim, A.F., Mazher, J., et al, 2020. Structural and Optical Characteristics of Highly UV-Blue Luminescent ZnNiO Nanoparticles Prepared by Sol-Gel Method. *Materials.* 13, 879.
- Flores, N.M., Pal, U., Galeazzi, R., et al, 2014. Effects of morphology, surface area, and defect content on the photocatalytic dye degradation performance of ZnO nanostructures. *RSC Adv.* 4, 41099–41110.
- Ghosh, S., Mith, T., Rana, S. et al., 2020. Nanofinishing of textiles for sportswear.

- Gokarneshan, N., Velumani, K., 2018. Significant trends in nano finishes for improvement of functional properties of fabrics. *Handbook of Renewable Materials for Coloration and Finishing*; Scrivener Publishing LLC, Beverly, MA, USA, pp. 387–434.
- Gross, E., Kornijów, R., 2002. Investigation on competitors and predators of herbivorous aquatic Lepidoptera (*Acentria ephemerella*) on submersed macrophytes in a large prealpine lake. *Internationale Vereinigung für theoretische und angewandte Limnologie: Verhandlungen*. 28, 721–725.
- He, W., Kim, H.-K., Wamer, W.G., et al, 2014. Photogenerated Charge Carriers and Reactive Oxygen Species in ZnO/Au Hybrid Nanostructures with Enhanced Photocatalytic and Antibacterial Activity. *J. Am. Chem. Soc.* 136, 750–757. <https://doi.org/10.1021/ja410800y>.
- Ijaz, U., Bhatti, I.A., Mirza, S., et al, 2017. Characterization and evaluation of antibacterial activity of plant mediated calcium oxide (CaO) nanoparticles by employing *Mentha pipertia* extract. *Mater. Res. Express* 4. <https://doi.org/10.1088/2053-1591/aa8603> 105402.
- Iuga, C., Alvarez-Idaboy, J.R., Vivier-Bunge, A., 2011. ROS initiated oxidation of dopamine under oxidative stress conditions in aqueous and lipidic environments. *J Phys Chem B*. 115, 12234–12246. <https://doi.org/10.1021/jp206347u>.
- Jiang, S., Lin, K., Cai, M., 2020. ZnO Nanomaterials: Current Advancements in Antibacterial Mechanisms and Applications. *Front. Chem.* 8. <https://doi.org/10.3389/fchem.2020.00580>.
- Johnson, D., Reeks, J.M., Caron, A., et al, 2022. Influence of Surface Properties and Microbial Growth Media on Antibacterial Action of ZnO. *Coatings* 12, 1648.
- Kadiyala, U., Turali-Emre, E.S., Bahng, J.H., et al, 2018. Unexpected insights into antibacterial activity of zinc oxide nanoparticles against methicillin resistant *Staphylococcus aureus* (MRSA). *Nanoscale* 10, 4927–4939.
- Kanjwal, M.A., Barakat, N.A., Sheikh, F.A., et al, 2010. Effects of silver content and morphology on the catalytic activity of silver-grafted titanium oxide nanostructure. *Fibers Polym.* 11, 700–709.
- Kawasaki, H., 2013. Surfactant-free solution-based synthesis of metallic nanoparticles toward efficient use of the nanoparticles' surfaces and their application in catalysis and chemo-/biosensing. *Nanotechnol. Rev.* 2, 5–25.
- Khalil, I.A., Troeger, C., Blacker, B.F., et al, 2018. Morbidity and mortality due to shigella and enterotoxigenic *Escherichia coli* diarrhoea: the Global Burden of Disease Study 1990–2016. *Lancet Infect. Dis.* 18, 1229–1240.
- Kostic, M.M., Milanovic, J.Z., Baljak, M.V., et al, 2014. Preparation and characterization of silver-loaded hemp fibers with antimicrobial activity. *Fibers Polym.* 15, 57–64.
- Kumar, A., Pandey, A.K., Singh, S.S., et al, 2011. Engineered ZnO and TiO₂ nanoparticles induce oxidative stress and DNA damage leading to reduced viability of *Escherichia coli*. *Free Radic. Biol. Med.* 51, 1872–1881.
- Lakshmi Prasanna, V., Vijayaraghavan, R., 2015. Insight into the mechanism of antibacterial activity of ZnO: surface defects mediated reactive oxygen species even in the dark. *Langmuir* 31, 9155–9162.
- Li, Q., Chen, S.L., Jiang, W.C., 2007. Durability of nano ZnO antibacterial cotton fabric to sweat. *J. Appl. Polym. Sci.* 103, 412–416.
- Li, G., Hu, T., Pan, G., et al, 2008. Morphology– function relationship of ZnO: polar planes, oxygen vacancies, and activity. *J. Phys. Chem. C* 112, 11859–11864.
- Li, N., Tian, Y., Zhao, J., et al, 2017. Efficient removal of chromium from water by Mn₃O₄@ ZnO/Mn₃O₄ composite under simulated sunlight irradiation: synergy of photocatalytic reduction and adsorption. *Appl Catal B* 214, 126–136.
- Li, M., Zhu, L., Lin, D., 2011. Toxicity of ZnO nanoparticles to *Escherichia coli*: mechanism and the influence of medium components. *Environ. Sci. Tech.* 45, 1977–1983.
- Liang, Y.-C., 2012. Growth and physical properties of three-dimensional flower-like zinc oxide microcrystals. *Ceram. Int.* 38, 1697–1702.
- Liew, K.B., Janakiraman, A.K., Sundarapandian, R., et al, 2022. A review and revisit of nanoparticles for antimicrobial drug delivery. *J Med Life.* 15, 328–335. <https://doi.org/10.25122/jml-2021-0097>.
- Liu, S., Lai, Y., Zhao, X., et al, 2019b. The influence of H₂O₂ on the antibacterial activity of ZnO. *Mater. Res. Express* 6, 0850c0856.
- Liu, J., Wang, Y., Ma, J., et al, 2019a. A review on bidirectional analogies between the photocatalysis and antibacterial properties of ZnO. *J. Alloy. Compd.* 783, 898–918.
- Masar, M., Ali, H., Guler, A.C., et al, 2023. Multifunctional bandgap-reduced ZnO nanocrystals for photocatalysis, self-cleaning, and antibacterial glass surfaces. *Colloids Surf A Physicochem Eng Asp* 656. <https://doi.org/10.1016/j.colsurfa.2022.130447> 130447.
- Muñoz-Bonilla, A., Fernández-García, M., 2015. The roadmap of antimicrobial polymeric materials in macromolecular nanotechnology. *Eur. Polym. J.* 65, 46–62.
- Naseem, T., Durrani, T., 2021. The role of some important metal oxide nanoparticles for wastewater and antibacterial applications: A review. *Environmental Chemistry and Ecotoxicology.* 3, 59–75. <https://doi.org/10.1016/j.eneco.2020.12.001>.
- Pasquet, J., Chevalier, Y., Couval, E., et al, 2014. Antimicrobial activity of zinc oxide particles on five micro-organisms of the Challenge Tests related to their physicochemical properties. *Int. J. Pharm.* 460, 92–100.
- Patil, A.H., Jadhav, S.A., More, V.B., et al, 2021. A new method for single step sonosynthesis and incorporation of ZnO nanoparticles in cotton fabrics for imparting antimicrobial property. *Chem. Pap.* 75, 1247–1257.
- Perelshtein, I., Lipovsky, A., Perkas, N., et al, 2015. The influence of the crystalline nature of nano-metal oxides on their antibacterial and toxicity properties. *Nano Res.* 8, 695–707.
- Pirzada, B.M., Dar, A.H., Shaikh, M.N., et al, 2021. Reticular-chemistry-inspired supramolecule design as a tool to achieve efficient photocatalysts for CO₂ reduction. *ACS Omega* 6, 29291–29324.
- Pirzada, B.M., Pushpendra, R.K., Kunchala, et al, 2019. Synthesis of LaFeO₃/Ag₂CO₃ nanocomposites for photocatalytic degradation of Rhodamine B and p-chlorophenol under natural sunlight. *ACS Omega* 4, 2618–2629.
- Prescott, S.C., Breed, R.S., 1910. The determination of the number of body cells in milk by a direct method. *J Infect Dis*, 632–640.
- Rahmat, M., Bhatti, H., Rehman, A., et al, 2021. Bionanocomposite of Au decorated MnO₂ via in situ green synthesis route and antimicrobial activity evaluation. *Arab. J. Chem.* 14, 103415.
- Ramirez-Canon, A., Medina-Llamas, M., Vezzoli, M., et al, 2018. Multiscale design of ZnO nanostructured photocatalysts. *PCCP* 20, 6648–6656.
- Ravikumar, S., Mani, D., Khan, M.R., et al, 2021. Ag-TiO₂@ Pd/C nanocomposites for efficient degradation of Reactive Red 120 dye and ofloxacin antibiotic under UV and solar light and its antimicrobial activity. *J. Environ. Chem. Eng.* 9, 106657.
- Ren, J., Wang, W., Sun, S., et al, 2011. Crystallography facet-dependent antibacterial activity: the case of Cu₂O. *Ind. Eng. Chem. Res.* 50, 10366–10369.
- Saleem, H., Zaidi, S.J., 2020. Sustainable use of nanomaterials in textiles and their environmental impact. *Materials.* 13, 5134.
- Shah, M.A., Pirzada, B.M., Price, G., et al, 2022. Applications of nanotechnology in smart textile industry: A critical review. *J. Adv. Res.*
- Sharma, N., Sharma, S., Sachdev, K., 2019. Effect of precursors on the morphology and surface area of LaFeO₃. *Ceram. Int.* 45, 7217–7225.
- Singh, R., Verma, K., Patyal, A., et al, 2019. Nanosheet and nanosphere morphology dominated photocatalytic & antibacterial properties of ZnO nanostructures. *Solid State Sci.* 89, 1–14.

- Sirelkhatim, A., Mahmud, S., Seeni, A., et al, 2015. Review on zinc oxide nanoparticles: antibacterial activity and toxicity mechanism. *Nano-micro letters*. 7, 219–242.
- Song, J., Wang, C., Hinestroza, J.P., 2013. Electrostatic assembly of core-corona silica nanoparticles onto cotton fibers. *Cellul*. 20, 1727–1736.
- Song, W., Zhang, J., Guo, J., et al, 2010. Role of the dissolved zinc ion and reactive oxygen species in cytotoxicity of ZnO nanoparticles. *Toxicol. Lett*. 199, 389–397.
- Sun, G., Cao, M., Wang, Y., et al, 2006. Anionic surfactant-assisted hydrothermal synthesis of high-aspect-ratio ZnO nanowires and their photoluminescence property. *Mater. Lett*. 60, 2777–2782.
- Sun, D., Siddiqui, M.O.R., Iqbal, K., 2019. Specialty testing techniques for smart textiles. *Smart Textile Coatings and Laminates*. Elsevier, pp. 99–116.
- Sun, Y., Wang, L., Yu, X., et al, 2012. Facile synthesis of flower-like 3D ZnO superstructures via solution route. *CrstEngComm* 14, 3199–3204.
- Taghipour, F., 2004. Ultraviolet and ionizing radiation for microorganism inactivation. *Water Res*. 38, 3940–3948.
- Tang, K., Gu, S.-L., Ye, J.-D., et al, 2017. Recent progress of the native defects and p-type doping of zinc oxide. *Chin. Phys. B* 26, 047702.
- Tudu, B.K., Sinhamahapatra, A., Kumar, A., 2020. Surface modification of cotton fabric using TiO₂ nanoparticles for self-cleaning, oil–water separation, antistain, anti-water absorption, and antibacterial properties. *ACS Omega* 5, 7850–7860.
- Ullah, N., Yasin, S., Abro, Z., et al, 2014. Mechanically robust and antimicrobial cotton fibers loaded with silver nanoparticles: Synthesized via Chinese holly plant leaves. *Int. J. Text. Sci.* 3, 1–5.
- Van Houdt, R., Michiels, C.W., 2005. Role of bacterial cell surface structures in *Escherichia coli* biofilm formation. *Res. Microbiol*. 156, 626–633.
- Vijayaraghavan, R., 2017. Chemical manipulation of oxygen vacancy and antibacterial activity in ZnO. *Mater. Sci. Eng. C* 77, 1027–1034.
- Wang, J., Wang, Z., Huang, B., et al, 2012. Oxygen vacancy induced band-gap narrowing and enhanced visible light photocatalytic activity of ZnO. *ACS Appl. Mater. Interfaces* 4, 4024–4030.
- Wang, J., Chen, R., Xiang, L., et al, 2018. Synthesis, properties and applications of ZnO nanomaterials with oxygen vacancies: a review. *Ceram. Int*. 44, 7357–7377.
- Wang, L., Hu, C., Shao, L., 2017b. The antimicrobial activity of nanoparticles: present situation and prospects for the future. *Int. J. Nanomed*. 12, 1227.
- Wang, S., Xu, D., Zhu, P., et al, 2022. Facile fabrication of antibacterial and fire-safety multifunctional cotton fabric with a triazine-phosphonate N-halamine. *Ind. Crop. Prod*. 186, 115261.
- Wang, D., Zhao, L., Ma, H., et al, 2017a. Quantitative analysis of reactive oxygen species photogenerated on metal oxide nanoparticles and their bacteria toxicity: the role of superoxide radicals. *Environ. Sci. Tech*. 51, 10137–10145.
- Wolanov, Y., Prikhodchenko, P.V., Medvedev, A.G., et al, 2013. Zinc dioxide nanoparticles: A hydrogen peroxide source at moderate pH. *Environ. Sci. Tech*. 47, 8769–8774.
- Wu, W., Zhao, W., Wu, Y., et al, 2019. Antibacterial behaviors of Cu₂O particles with controllable morphologies in acrylic coatings. *Appl. Surf. Sci*. 465, 279–287.
- Xia, T., Kovoichich, M., Liong, M., et al, 2008. Comparison of the mechanism of toxicity of zinc oxide and cerium oxide nanoparticles based on dissolution and oxidative stress properties. *ACS Nano* 2, 2121–2134.
- Xu, B., Cai, Z., 2008. Fabrication of a superhydrophobic ZnO nanorod array film on cotton fabrics via a wet chemical route and hydrophobic modification. *Appl. Surf. Sci*. 254, 5899–5904.
- Xu, X., Chen, D., Yi, Z., et al, 2013. Antimicrobial mechanism based on H₂O₂ generation at oxygen vacancies in ZnO crystals. *Langmuir* 29, 5573–5580.
- Xu, Q., Zheng, W., Duan, P., et al, 2019. One-pot fabrication of durable antibacterial cotton fabric coated with silver nanoparticles via carboxymethyl chitosan as a binder and stabilizer. *Carbohydr. Polym.* 204, 42–49.
- Yang, H., Zhu, S., Pan, N., 2004. Studying the mechanisms of titanium dioxide as ultraviolet-blocking additive for films and fabrics by an improved scheme. *J. Appl. Polym. Sci.* 92, 3201–3210.
- Yemmireddy, V.K., Hung, Y.C., 2017. Using photocatalyst metal oxides as antimicrobial surface coatings to ensure food safety—Opportunities and challenges. *Compr. Rev. Food Sci. Food Saf.* 16, 617–631.
- Zhang, L., 2008. *Prog Nat Sci-Mater*. V18, 939.
- Zhang, W., Lee, S., McNear, K.L., et al, 2014a. Use of graphene as protection film in biological environments. *Sci. Rep.* 4, 1–8.
- Zhang, X., Qin, J., Xue, Y., et al, 2014b. Effect of aspect ratio and surface defects on the photocatalytic activity of ZnO nanorods. *Sci. Rep.* 4, 1–8.
- Zhang, H., Wu, R., Chen, Z., et al, 2012. Self-assembly fabrication of 3D flower-like ZnO hierarchical nanostructures and their gas sensing properties. *CrstEngComm* 14, 1775–1782.
- Zhou, H., Zhang, H., Wang, Y., et al, 2015. Self-assembly and template-free synthesis of ZnO hierarchical nanostructures and their photocatalytic properties. *J. Colloid Interface Sci.* 448, 367–373.
- Zille, A., Almeida, L., Amorim, T., et al, 2014. Application of nanotechnology in antimicrobial finishing of biomedical textiles. *Mater. Res. Express* 1, 032003.